Broadband Variable Radial Waveguide Power Combiner Using Multi-Section Impedance Matching Technique

Gang Xu, Xue-Song Yang, Jia-Lin Li, and Zhi-Ming Tian

School of Physical Electronics
University of Electronic Science and Technology of China, Chengdu, 610054, China
xsyang@uestc.edu.cn

Abstract ― An L-band spatial variable radial waveguide power combiner with broad bandwidth and high power capacity is proposed. By adopting several techniques simultaneously, including multi-section impedance matching probes, grounded disc, and axial slots, the performance of the power combiner is improved. The parameters of the combiner are calculated, simulated and tested. It has a measured operation bandwidth ranging from 1.2 GHz to 2 GHz with VSWRs less than 1.4 at all ports. The extra insertion losses between the input ports and output port are less than 0.3 dB and the isolation between the input ports is better than 15 dB. The power capacity can reach 600 W and the combining efficiency achieves 90 %. The results from calculation, simulation, and measurement reasonably agree with each other.

Index Terms ― Broadband power combiner, microwave components, multi-section impedance matching, spatial power combiner, and variable radial waveguide.

I. INTRODUCTION

The power combiner/divider has been used extensively in wireless communications and Radar systems [1-4]. Recently, a lot of attention has been paid to the power combiner/divider with high efficiency, high power capacity and broadband characteristics. However, some traditional power combiner/divider, such as Wilkinson power divider, Lange coupler, and branch line coupler are limited by their low combining efficiency [1], while the rectangular waveguide circuits [3-5] are restricted by the difficulty of achieving wide bandwidth due to the cut-off frequency. Besides, quasi-optical cavity [6] and oversized coaxial waveguide power combiner/divider suffer from large insertion loss, although they can achieve wide bandwidth [7, 8]. Compared with the aforementioned ones, radial waveguide combiner/divider has advantages of easy fabrication, wide bandwidth, and high combining efficiency [9-11]. However, there still exist some shortcomings, such as excess insertion losses and poor isolation performance between ports.

In this paper, a three-way spatial power combiner is proposed based on the variable radial waveguide. The developed combiner exhibits good insertion losses between input and output ports, as well as enhanced port-to-port isolation between input ports. Besides, good return losses are given at all ports. In order to improve the port-to-port isolation between input ports, three axial slots are etched on the cavity sidewall. Furthermore, a grounded disc on the wall of the cavity is used to improve the port-to-port isolation performance, as well as the impedance matching. Besides, multi-section matching technology is adopted to improve the impedance matching of the combiner [12]. The paper is organized as follows, section II introduces the design of the power combiner. Section III gives the calculation, simulation, and measurement results. Conclusion is provided in section IV.

II. DESIGN OF THE POWER COMBINER

The proposed three-way spatial power combiner is shown in Fig. 1. The combiner

Submitted On: July 24, 2012
Accepted On: Mar. 18, 2013

consists of a radial waveguide with three peripheral coaxial probes, used as input ports, and one center coaxial probe, used as output port. Each coaxial probe has a cylindrical shape, including three stepped matching sections. The multi-section impedance transformer probe is advantageous to improve the impedance matching of each port [13]. A grounded disc with diameter d_t, located on the wall of the waveguide at the center of the peripheral probes side, is introduced to improve the port-to-port isolation, as well as improve the impedance matching [12]. Furthermore, three axial slots etched on the cylinder sidewall of the radial waveguide, are used to improve the isolation performance between the input ports [14]. According to the perturbation theory, the grounded disc opposite to the output probe weakens the coherent electric field on the output probe, while the axial slots on the sidewall weaken the coherent electric field on the input probes. Consequently, the isolation performance is improved by adopting these two structures substantially. The interaction between probes (including coupling and interference) can be analyzed based on the generalized balance theory [15, 16].

The three peripheral probes are identical and radially distributed at one side of the radial waveguide. Consequently, one of the input coaxial probes can be taken for analysis because of the structural symmetry. The longitudinal section including the output port and one input port is shown in Fig. 1 (b). The probes are fixed in the cavity with the use of poly-tetra-fluorethylene (PTFE). The three matching sections of the output probe are named Matching Sections -1, -2, and -3, and those of the input probe are named Matching Sections -4, -5, and -6, respectively. The lengths and diameters of Matching Sections -1 to -6 are l_1 to l_6 and d_1 to d_6, respectively, as shown in Fig. 1 (b). In order to design the combiner, the distance R_g between the axes of the input and output probes, as shown in Fig. 1 (b), should be calculated. This can be done based on the theory of parallel coupled transmission lines. After that, the output probe and one input probe are analyzed as a two-port network. By this way, the equivalent impedance of each probe can be calculated. According to the multi-section impedance matching theory, the structural parameters of the input and output probes can be obtained, as formulated below.

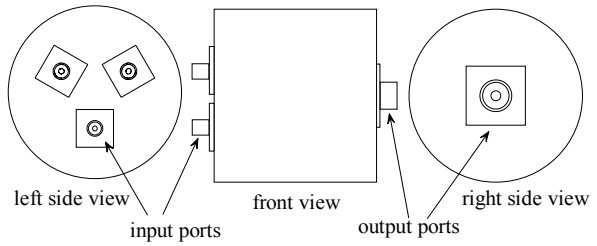

(a) Outside view.

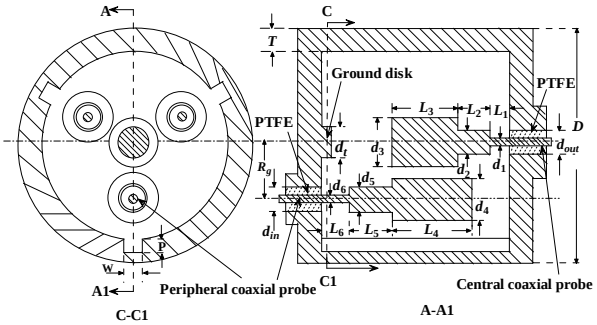

(b) Cross-section view and longitudinal-section view.

Fig. 1. Structure of the three-way variable radial-waveguide power combiner.

For the sake of analysis, each matching section of the probe can be viewed as a virtual coaxial line (inner diameter of d_i and outer diameter of D_i). The inner diameter of the virtual coaxial line is actually the diameter of the matching section. Due to the interaction between the input and output probes, the outer conductor diameter D_i is an equivalent value or calculated value, which is given by the following expressions [10]

$$\begin{cases} D_i = k_i(B-2T) & (i=1,2) \\ D_i = 2R_g & (i=3,4), \\ D_i = k_i(B-2T-2R_g) & (i=5,6) \end{cases} \quad (1)$$

where B is the diameter of the cavity, T is the thickness of the cavity wall, R_g is the distance between input and output probes, and k_i is the weighting factor, which is given as

$$k_i = \frac{B-2T-d_i}{2R_g} \quad (i=1,2,5,6). \quad (2)$$

The equivalent impedance of each matching section of each probe can be expressed as,

$$Z_i = R_i + jX_i \quad (i=1,2,...,6) \quad (3)$$

where R_i and X_i are the real and imaginary parts of the equivalent impedance, respectively.

The real part of the equivalent impedance of the probe is actually the characteristic impedance of the coaxial line, which can be obtained by

$$R_i = \frac{60}{\sqrt{\varepsilon_0}} \frac{d_i}{D_i} \quad (i = 1, 2, \cdots, 6), \tag{4}$$

where d_i is the inner conductor diameter, and ε_0 is the vacuum dielectric constant.

According to the parallel lines coupling theory, the mutual coupling between input and output probes can be taken as mutual impedance, and is further equivalent to the imaginary part of the input impedance of the probe. Since Matching Sectoin-1 is more independent, the imaginary part of its input impedance can be calculated as [10]

$$X_1 = \frac{\mu_0 l_1}{8\pi}, \tag{5}$$

where μ_0 is the vacuum permeability.

Since the spacing between Matching Sections-2, -3, and Section-4 are small, there exists strong coupling between them and then electrical coupling plays a major role. The imaginary part of the input impedance is given as [10]

$$X_i = 2\pi\varepsilon_0 \left(\frac{1}{\ln\frac{D_i}{d_3}} - \frac{1}{\ln\frac{D_i}{d_4}}\right) P_i \quad (i = 2, 3, 4), \tag{6}$$

where P_i is the length of the common part of two parallel sections.

The radii of Matching Sections-5 and -6 are much smaller than the distance between two input probes. As a result, the magnetic coupling plays a major role and the imaginary part of the input impedance can be calculated as [10]

$$X_i = \frac{\mu_0 d_i^4 \pi}{32\left[\left(\frac{D_i}{2}\right)^2 + \left(\frac{d_i}{2}\right)^2\right]^{3/2}} \quad (i = 5, 6). \tag{7}$$

According to the multi-section impedance matching theory [17], the reflection coefficient of each matching section can be expressed as,

$$\Gamma_{si} = \frac{Z_i - Z_{i-1}}{Z_i + Z_{i-1}} \quad (i = 2, 3) \tag{8}$$

$$\Gamma_{si} = \frac{Z_i - Z_{i+1}}{Z_i + Z_{i+1}} \quad (i = 4, 5), \tag{9}$$

$$\Gamma_{si} = \frac{Z_i - Z_0}{Z_i + Z_0} \quad (i = 1, 6), \tag{10}$$

where Z_i is the equivalent impedance of Matching Section-i and Z_0 is 50 ohm.

In order to describe the combiner more clearly, the output port is named Port-1, and the three input ports are named Ports-2, -3, and -4, respectively. The reflection coefficient of the port can be calculated by,

$$\Gamma_{p1} = \Gamma_{s1} + (1-\Gamma_{s1})\Gamma_{s2} + \left[1-\left(1-\Gamma_{s1}\right)\Gamma_{s2}\right]\Gamma_{s3} \tag{11}$$

$$\Gamma_{pj} = \Gamma_{s6} + (1-\Gamma_{s6})\Gamma_{s5} + \left[1-\left(1-\Gamma_{s6}\right)\Gamma_{s5}\right]\Gamma_{s4} \quad (j=2, 3, 4), \tag{12}$$

where Γ_{si} is the reflection coefficient of the Matching Sections-i (i=1,2,…,6), and Γ_{pj} is the total reflection coefficient of port j (j = 1, 2, 3 and 4), when the reflection coefficient of each Matching Section is independent.

Then, the VSWR and input impedance of each port can be calculated by,

$$VSWR_j = \frac{1+\left|\Gamma_{pj}\right|}{1-\left|\Gamma_{pj}\right|} \quad (j=1, 2, 3, 4). \tag{13}$$

Consequently, with the given VSWR, the dimensions of the probes can be calculated conversely.

III. PERFORMANCE OF THE COMBINER

A. Impedance matching, insertion loss, and isolation

A combiner is designed and fabricated with the structural parameters listed in Table 1. The performance of the combiner is simulated by using Ansoft's HFSS. The fabricated combiner, as shown in Fig. 2, is measured with the use of an HP vector network analyzer HP8753C. The simulated and measured parameters are shown in Fig. 3.

Basically, performances of the three input ports are the same, thus only one input port VSWR is given. As shown in Fig. 3 (a), the simulated VSWRs of both Port-1 and Port-2 are less than 1.22 ($|S_{11}|$ = -20 dB) within the bandwidth from 1.2 GHz to 2 GHz, while the measured ones are less than 1.4 ($|S_{11}|$ = -15.5 dB), indicating good impedance matching at both input and output ports. The phase imbalance of the three input ports is better than 1 degree, which is shown in Fig. 3 (b), where the phase of S_{41} is taken as a reference.

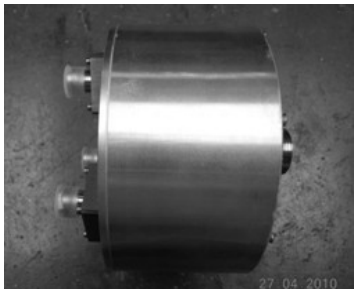

Fig. 2. Fabricated combiner.

Table 1: Dimensions of the power combiner (unit: mm).

l_1	l_2	l_3	l_4	l_5	l_6
26	13	6	25	14	10
d_1	d_2	d_3	d_4	d_5	d_6
8	16	36	24	8	4
B	T	d_{in}	d_{out}	R_g	d_t
150	7.5	9.2	18	46	12

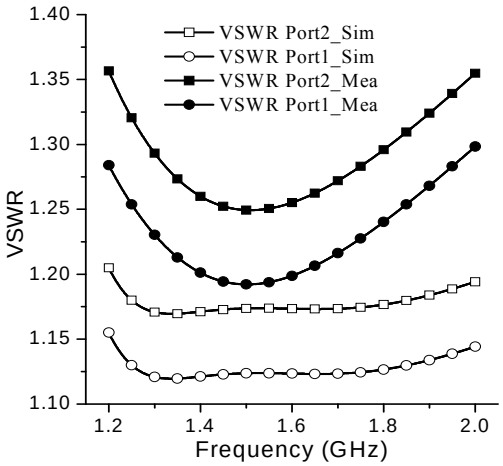

(a) VSWR.

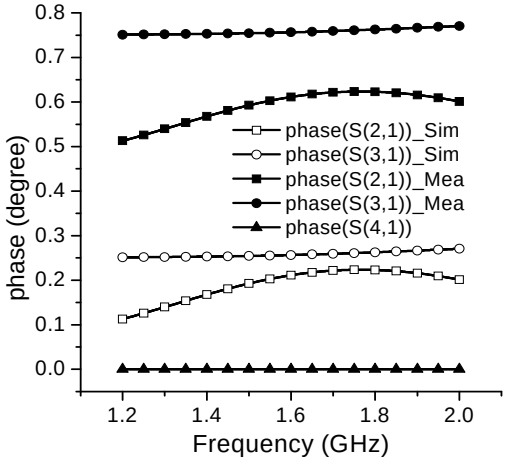

(b) Phase.

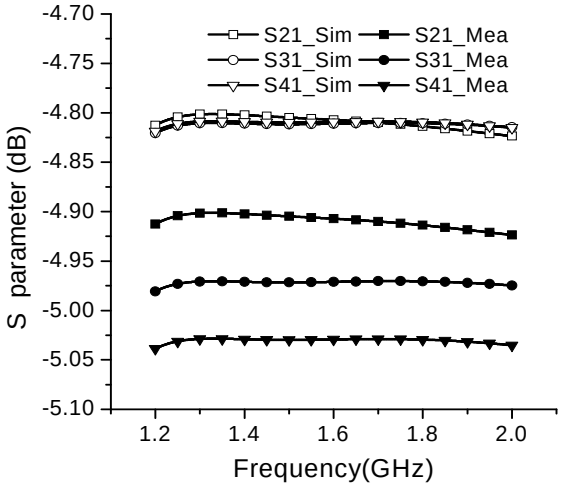

(c) S-parameters between the input ports and output port.

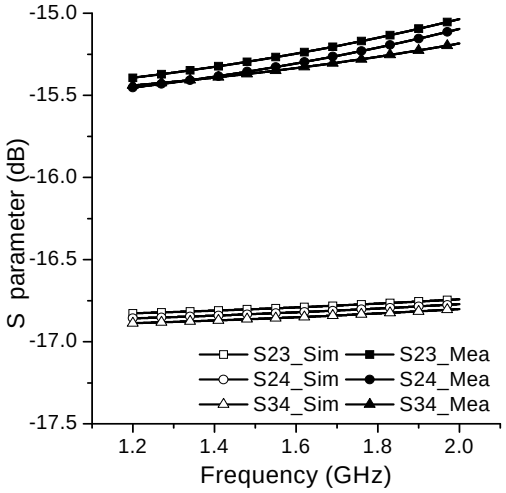

(d) S-parameters between the input ports.

Fig. 3. Simulated and measured results.

Figure 3 (c) presents the power dividing performance of the three ways. The simulation results show that the insertion loss of each way is very close to the theoretical value of 4.78 dB (10log(1/3) = -4.78), while the test curves range between 4.9 dB and 5.05 dB, revealing a maximum in-band additional insertion losses being less than 0.3 dB. Figure 3 (d) shows both the simulated and the measured isolation between any two input ports. The values are better than 15 dB, which meet the design requirements.

From Figure 3, it is clear that the three-way power combiner show a good equalization of power division among three input ports while

maintaining relatively low return loss at each port over a wide bandwidth.

Based on the structural parameters of the combiner, the S-parameters can be calculated, as listed in Table 2. It can be found that the calculated results are consistent with the simulated and measured ones.

Table 2: Calculated S-parameters.

VSWR		S_{21} (dB)	S_{31} (dB)	S_{41} (dB)	S_{23} (dB)	S_{24} (dB)
input port	output port					
1.2	1.25	- 4.8	- 4.8	- 4.9	- 15	- 15

B. Efficiency and power capacity

Since the power capacity of the combiner is determined by the heat breakdown voltage of PTFE [18], according to the theorem of energy storage capacitor, the total capacity of the combiner is calculated by

$$W_e = \frac{3 \times \varepsilon_r \times D^2}{2}, \tag{14}$$

where ε_r is the dielectric constant of PTFE and D is the electric displacement vector. The calculated power capacity W_e is higher than 600 Watt according to the simulation.

The combining efficiency can be calculated by,

$$\eta = \frac{P_{out}}{P_{in}} \tag{15}$$

where P_{out} and P_{in} are the output power and input power, respectively. The measured output and input powers are 540 Watt and 600 Watt, respectively. Consequently, the combining efficiency of this combiner reaches 90 %.

IV. CONCLUSION

In this article, an L-band broadband power combiner has been designed based on variable radial waveguide spatial power combining technology. The developed combiner exhibits good insertion losses between the input and output ports, as well as enhanced port-to-port isolation between input ports. Three axial slots on the cavity sidewall and a grounded disc on the wall of cavity have improved the port-to-port isolation between input ports. Moreover, good VSWR has been obtained with the use of multi-section impedance matching. The tested operating bandwidth ranges from 1.2 GHz to 2 GHz with VSWRs less than 1.4 at all ports. The extra insertion losses between the input and output ports are less than 0.3 dB and the isolation between the input ports is better than 15 dB. The power capacity has reached 600 W and the combining efficiency has achieved 90 %. Results from experiments have validated the design expectation with good agreement.

ACKNOWLEDGMENT

This work was supported by the Natural Science Foundation of China (61271027, 61271025).

REFERENCES

[1] M. Belaid, R. Martinez, and K. Wu, “A mode transformer using fin-line array for spatial power -combiner applications,” *IEEE Transactions on Microwave Theory and Techniques*, vol. 52, no. 4, pp. 1191-1198, 2004.

[2] D. I. L. de Villiers, P. W. Van der Walt, and P. Meyer, “Design of a ten-way conical transmission line power combiner,” *IEEE Transactions on Microwave Theory and Techniques*, vol. 55, no. 2, Part 1, pp. 302-308, 2007.

[3] J. P. Becker and A. M. Oudghiri, “A planar probe double ladder waveguide power divider,” *IEEE Microwave and Wireless Components Letters*, vol. 15, no. 3, pp. 168-170, 2005.

[4] P. Jia, L. -Y. Chen, A. Alexanian, and R. A. York, “Broad-band high-power amplifier using spatial power- combining technique,” *IEEE Transactions on Microwave Theory and Techniques*, vol. 51, no. 12, pp. 2469-2475, 2003.

[5] S. C. Ortiz, J. Hubert, L. Mirth, E. Schlecht, and A. Mortazawi, “A high-power Ka-band quasi-optical amplifier array,” *IEEE Transactions on Microwave Theory and Techniques*, vol. 50, no. 2, pp. 487-494, 2002.

[6] M. P. Delisio and R. A. York, “Quasi-optical and spatial power combining,” *IEEE Transactions on Microwave Theory and Techniques*, vol. 50, no. 3, pp. 929-936, 2002.

[7] P. Jia, L. -Y. Chen, A. Alexanian, and R. A. York, “Multioctave spatial power combining in oversized coaxial waveguide,” *IEEE Transactions on Microwave Theory and Techniques*, vol. 50, no. 5, pp. 1355-1360, 2002.

[8] K. Song, Y. Fan, and X. Zhou, “Broadband millimeter-wave passive spatial combiner based on coaxial waveguide,” *IET Microwaves, Antennas and Propagation*, vol. 3, no. 4, pp.

607-613, 2009.

[9] K. Song, Y. Fan, and Z. He, "Broadband radial waveguide spatial combiner," *IEEE Microwave and Wireless Components Letters*, vol. 18, no. 2, pp. 73-75, 2008.

[10] D. M. Pozar, *Microwave Engineering*, John Wiley & Sons, 3rd Edition, pp. 244-250, 2005.

[11] Y. -P. Hong, D. F. Kimball, P. M. Asbeck, J. -G. Yook, and L. E. Larson, "Single-ended and differential radial power combiners implemented with a compact broadband probe," *IEEE Transactions on Microwave Theory and Techniques*, vol. 58, no. 6, pp. 1565-1568, 2010.

[12] M. E. Bialkowski, "Analysis of a coaxial-to-waveguide adaptor including a discended probe and a tuning post," *IEEE Transactions on Microwave Theory and Techniques*, vol. 43, no. 2, pp. 344-349, 1995.

[13] R. E. Collin, *Fundamentals of Microwave Engineering*, Wiley-IEEE Press, 2nd Edition, pp. 64-179, 2000.

[14] Y. -P. Hong, D. F. Kimball, P. M. Asbeck, J. -G. Yook, and L. E. Larson, "Switch-controlled multi-octave bandwidth radial power divider/combiner," *IEEE Microwave Symposium Digest (MTT)*, pp. 932-935, 2010.

[15] C. M. Montiel, "Sonnet EM simulation of printed Baluns using PCB data extraction," *27th Annual Review of Progress in Applied Computational Electromagnetics*, Williamsburg, Virginia, pp. 357 -362, March 27-31, 2011.

[16] C. M. Montiel, "Folded Marchand Balun Design and Validation Using Sonnet," *28th Annual Review of Progress in Applied Computational Electromagnetics*, Columbus, Ohio, pp. 680-685, April 10-14, 2012.

[17] G. L. Matthaei, L. Young, and E. M. T. Jones, *Microwave Filter Impedance-Matching Networks and Coupling Structures*, McGraw-Hill book Co., Inc., New York, pp. 126-128, 1985.

[18] H. R Zeller, "Breakdown and pre-breakdown phenomena in solid dielectrics," *IEEE Transactions on Electrical Insulation*, vol. 22, no. 2, pp. 115-122, 1987.

Gang Xu received the M.Sc. degree from UESTC, Chengdu, China. He was with the UESTC and now is with the CETC. His current interest is microwave circuits.

Xue-Song Yang received the Ph.D. degree in Radio Physics from UESTC, Chengdu, China. She joined the UESTC in 2002, where she is currently an Associate Professor. She has been a research fellow at the City University of Hong Kong, a Visiting Scholar at the University of Southern California. Her current research interests include reconfigurable antennas, UWB antennas and wireless channel modeling.

Jia-Lin Li received the M.Sc. degree from UESTC, Chengdu, China, in 2004, and the Ph.D. degree from the City University of Hong Kong, Hong Kong, in 2009, both in Electronic Engineering. Since Sept. 2009, he has been with the Institute of Applied Physics, School of Physical Electronics, UESTC, where he is currently a Professor. His research interests include the high performance active / passive microwave / millimeter-wave antennas, circuits and systems realized on PCB, multilayer PCB, LTCC, etc.

Zhi-Ming Tian received the B.Sc. degree in Physics form Tangshan Normal University, Tangshan, China, in 2009, and the Master degree from UESTC, Chengdu, China in 2012. His current research interests include wireless channel modeling and antennas design.